

The Structure of the Large Cosmic-Ray Air Showers

ROBERT W. WILLIAMS

*Physics Department and Laboratory for Nuclear Science and Engineering,
Massachusetts Institute of Technology, Cambridge, Massachusetts*

(Received August 24, 1948)

A series of experiments on cosmic-ray air showers is described. Four "fast" ionization chambers, with electronic coincidence and photographic recording of pulse height, were used to investigate the structure of these showers in detail, at mountain altitudes. The experiments show that the showers have the structure characteristic of electron cascades. There is no evidence for unusually narrow showers. If the showers originate from the decay of neutral mesons, these mesons must be produced either singly, or in groups whose total angular divergence is not greater than $\sim 10^{-4}$ radian.

The frequency of occurrence of showers which have particle density greater than ρ -particles per square meter at the point of observation is shown to be $1.05(460/\rho)^{1.5}$

hr.^{-1} , $300 < \rho < 2000$ particles/m², at 3050-m elevation. This frequency is also given for two points of observation with various distances separating them. Data on the angular distribution of the showers at 3050 m and the altitude variation between 3050 m and 4300 m are presented. The results of some theoretical calculations on altitude and angular variation are given, but they are not sufficiently accurate to indicate clearly the nature of the primary event which causes these showers. Absolute rates for the number of showers of a certain size, and for the number of primary events, are presented.

Twenty-seven showers of more than 10^{16} -ev total energy were recorded.

I. INTRODUCTION

LARGE cosmic-ray showers, often called "Auger showers" or "extensive showers," were discovered by Geiger-tube coincidence methods.^{1,2} They have also been investigated with cloud chambers^{3,4} and ionization chambers.⁵⁻⁷ Most of the Geiger-tube experiments seem to be in general agreement with the cascade theory of multiplication of high energy electrons and photons.^{3,8-12} The relation between theory and experiment is somewhat indirect, however; all Geiger-tube counting rates are averages over the local particle-density spectrum, which itself is an integral over space and over an assumed "primary" electron spectrum.

The ionization chamber has the advantage of making a direct measurement of the particle density in each shower. The experiments of

Lewis,^{5,7} using coincidence between two low pressure ionization chambers, have been interpreted as showing complete disagreement with the cascade theory,¹³ and the question has been raised whether the large air showers have an entirely different structure.¹⁴

Recent advances in experimental technique have made it possible to use pulse ionization chambers with quantitative electron collection as instruments of high sensitivity and microsecond time resolution.¹⁵ The present experiments make use of the new techniques to investigate in greater detail the structure of these air showers. In particular it proved feasible, by the simultaneous use of four pulse ionization chambers, to obtain direct information on the structure of an individual shower.

II. METHOD AND APPARATUS

A recent publication of this laboratory,¹⁶ hereafter referred to as BHRW, describes the ioniza-

¹ P. Auger, R. Maze, and T. Grivet-Meyer, *Comptes rendus* **206**, 1721 (1938).

² K. Schmeiser and W. Bothe, *Ann. d. Physik* **32**, 161 (1938).

³ P. Auger, R. Maze, P. Ehrenfest, and A. Freon, *J. de Phys. et rad.* **1**, 39 (1939).

⁴ J. Daudin, *J. de Phys. et rad.* **7**, 302 (1945).

⁵ L. Lewis, *Phys. Rev.* **67**, 228 (1945).

⁶ R. Lapp, *Phys. Rev.* **69**, 321 (1946).

⁷ K. L. Kingshill and L. Lewis, *Phys. Rev.* **69**, 159 (1946).

⁸ N. Hilberry, *Phys. Rev.* **60**, 1 (1941).

⁹ G. Cocconi, A. Loverdo, and V. Tongiori, *Phys. Rev.* **70**, 846 (1946).

¹⁰ H. Kraybill and P. Ovrebø, *Phys. Rev.* **72**, 351 (1947).

¹¹ G. Molière, *Cosmic Radiation*, ed. by W. Heisenberg (Dover Publications, New York, 1946), Ch. 3.

¹² H. W. Lewis, *Phys. Rev.* **73**, 1341 (1948).

¹³ L. Wolfenstein, *Phys. Rev.* **67**, 238 (1945).

¹⁴ Evidence has also been found, by counter experiments, for non-cascade radiation (penetrating particles) associated with air showers, but the number of these particles constitutes a very small fraction of the total number of shower particles, and some may be generated locally in the absorber. Cf. G. Cocconi and K. Greisen, *Phys. Rev.* **74**, 62 (1948).

¹⁵ Cf. B. Rossi and H. S. Staub, *Ionization Chambers and Counters*, Vol. 2 of the Los Alamos Technical Series, in print.

¹⁶ H. S. Bridge, W. E. Hazen, B. Rossi, and R. W. Williams, *Phys. Rev.* **74**, 1083 (1948).

tion chambers and auxiliary apparatus used by us, and discusses the application of ionization chambers to cosmic-ray measurements. Therefore, we shall describe only the main points of the method here, referring the reader to that paper for details.

1. Theory of the Ionization Chamber

An ionization chamber gives a signal which is directly related to the number of ion-pairs created in it. It is particularly appropriate for studying the particle density of showers of high energy particles, for this reason: the energy loss by collision which is experienced by a particle of electronic charge in matter is nearly a function of velocity alone.¹⁷ The number of ion-pairs created, per unit path length, is approximately proportional to the energy loss (and different for different materials). Therefore, a relativistic particle (velocity nearly c) will have a specific ionization almost independent of its mass and energy. Let this average specific ionization be j ion-pairs per gram per square centimeter, in the gas of the ionization chamber. If the ionization chamber is traversed by a shower whose particle density at any point is ρ particles per square centimeter, the number of ion-pairs created in the chamber is

$$N = j\delta \int_S \rho l dS,$$

where S is the area of the chamber perpendicular to the shower direction, l the length of path which a shower particle has in the chamber, and δ the density of the gas. If ρ is nearly constant over the area of the chamber, we obtain the relation $N = j\delta v\rho$ (where v is the chamber volume) which shows that the ionization chamber signal is a direct measure of the particle density in the shower.

The relation between the number of ion-pairs N which is released in the ionization chamber and the resulting change in potential difference of the electrodes is discussed in BHRW. (It should be noted that we are not interested in the average ionization current, but only in the sudden bursts of ionization, and resulting voltage pulses, connected with specific events.) In the chambers

used, the negative ions are electrons which are all collected within 7×10^{-6} second, and the output of the fast amplifiers is essentially proportional to the change in potential caused by the motion of the electrons alone. In a cylindrical ionization chamber with (positive) inner electrode of radius a and outer electrode of radius b , this change in potential is a fraction $f = \ln(r/a) / \ln(b/a)$ of the change caused by collecting the whole charge, if the electron is released at distance r from the axis. We may assume that the showers to be observed will leave an approximately uniform density of ionization in the chamber, so we find upon integrating the above expression over the chamber volume that the fraction of total potential change caused by electron motion is

$$f = b^2 / (b^2 - a^2) - 1 / (2 \ln(b/a)).$$

2. Calibration of Ionization Chambers

The ionization chambers used in this work are described in detail in BHRW. They were cylindrical, with outer electrode 7.45 cm, inner electrode 0.0635 cm, and active length 53 cm; they were filled with five atmospheres of specially purified argon. A thin source of polonium alpha-particles was permanently installed at the inside surface of the outer electrode.

The charge released by a polonium alpha-particle is $5.3 \times 10^6 e / W_0$, where W_0 is the average energy to produce an ion pair. The fraction of change in potential due to electron motion is unity in this case, because the entire charge is released very close to the wall of the ionization chamber. In Section 1, it was shown that the charge induced, when a shower of particle-density ρ strikes the ionization chamber, is $Ne = j\delta v\rho e$; the fraction of the corresponding change in potential which is due to electron motion is f . Thus if V is the change of potential due to a shower of particle-density ρ , and V_α is the change in potential caused by an alpha-particle,

$$\rho = 5.3 \times 10^6 V / fjW_0\delta v V_\alpha.$$

One correction is necessary. The brass walls of the ionization chamber, though only 0.7 g cm^{-2} thick, will change the density of shower particles slightly, mainly by materialization of photons.

¹⁷ B. Rossi and K. Greisen, Rev. Mod. Phys. **13**, 240 (1941).

Bethe¹⁸ has calculated the effect for a thin wall, and finds multiplication by a factor

$$1 + 2(1 - 7.2/Z)t/X_0,$$

where t is the thickness, Z is the atomic number, and X_0 the "radiation length" of cascade theory. For brass, $Z=29.2$, $X_0=13.3$ g cm⁻², so the multiplication would be 1.08 for our chamber, except that rays off the axis of the chamber see a greater thickness of material. This means that $t_{\text{effective}}$ is greater than t ; the factor proves to be $4/\pi$ if all the ions are collected. Electron collection complicates the matter, but an upper limit can be shown to be $\pi/2$. We take an intermediate value of 1.5, which makes the final multiplication factor 1.12. (Most showers prove to be nearly vertical at the altitude of these experiments, so the variation of t_{eff} because of inclination of the shower along the cylinder axis is ignored.)

The product jW_0 is just the average energy loss of a shower particle in one gram per square centimeter of the ionization chamber gas. If the chamber were filled with air, the value of the energy loss would be that used by the cascade theory. Since we have argon, but with particles of energy distribution corresponding to air, we

use the energy loss in argon of an electron of 10^8 ev, the average energy of cascade electrons in air.¹⁹ This is¹⁷ $jW_0 = 2.1 \times 10^6$ ev g⁻¹ cm². For our chambers $f=0.90$, $d=0.0083$ g cm⁻³, $v=2320$ cm³, and it is convenient to measure V in terms of V_c , a calibration voltage pulse applied to the high-voltage electrode (cf. BHRW). We find that $V_c=4.25$ millivolts corresponds to a polonium alpha-particle, so

$$\rho = 5.3 \times 10^6 \times 10^4 V_c / 1.12 \times 0.90 \times 2.1 \\ \times 10^6 \times 0.0083 \times 2320 \times 4.25 = 308 V_c,$$

where ρ is particles per square meter, and V_c is measured in millivolts.

3. Electronic Equipment

Figure 1 is a block diagram of the electronic equipment used to obtain data with the four ionization chambers. Each chamber is connected, through its own amplifier, to its own cathode-ray tube which is normally quiescent. In addition, each amplifier output is fed into an addition circuit, which is actuated whenever any two of the four chambers give pulses larger than a certain (adjustable) amount at the same time. When this circuit is actuated, it fires the sweeps

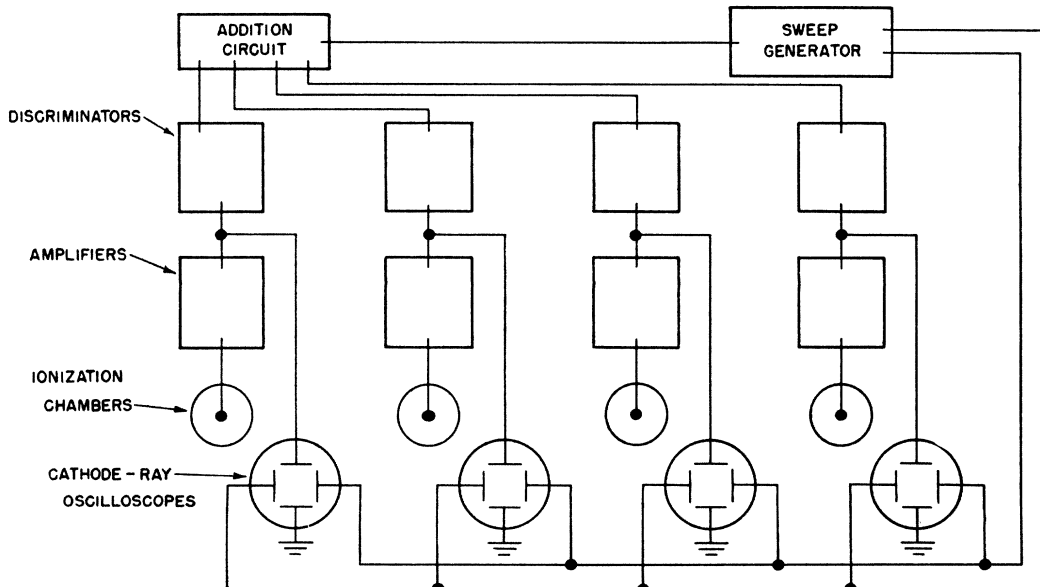


FIG. 1. Block diagram of the electronic circuits.

¹⁸ Private communication.

¹⁹ As indicated in the earlier discussion, jW_0 is not sensitive to this choice, and, in fact, the formulas for particle density will be approximately correct for any kind of shower with very high energy particles.

on the four cathode-ray tubes, thus giving a record of what is happening in each ionization chamber at that instant. Thus the oscilloscopes only sweep when a coincidence of a certain magnitude occurs, and they report, at that instant, on all four chambers, even though only two need to be giving pulses. The oscilloscope traces are recorded by a 16-mm movie camera. The film moves slowly and continuously, shutter always open, and whenever a shower of sufficient size strikes the chambers, the four sweeps fire and leave a record of the shower at that point of the film. Figure 2 shows a record of a shower.

The resolving time of the addition circuit which fires the sweep was 25 microseconds. Since the data are obtained from examination of the film, and the pulses rise in 7 microseconds, the true resolving time for the apparatus is that for which the pulses appear to be simultaneous, i.e., about 7 microseconds. The accidental rate—arising mostly from the alpha-particle source—was under 1 percent in all experiments.

III. EXPERIMENTAL PROCEDURE

1. Calibration and Routine Checks

Before each run the bias of the individual discriminators was set by means of the calibration pulser. Thus, for example, by setting the bias to correspond to $V_c = 2$ millivolts, only those events would be selected in which at least two



FIG. 2. Photographic record of a large air shower. Each of the four oscilloscope traces corresponds to one ionization chamber; the height of the pulse at the beginning of each trace is a measure of the particle density at that chamber. Total time of the sweep is 90 microseconds.

chambers had pulses corresponding to at least 616 particles per square meter density in their vicinity. A calibration record was then obtained by applying known calibration pulses of, for example, 2, 5, 10, and 20 millivolts to the chambers, and photographing the resultant oscilloscope traces. The calibration was repeated, and biases checked, at the end of each run. The stability of the amplifiers and discriminators was in this way found to be quite adequate.

This electrical calibration does not check on the possibility that the chamber leaks or the filling become contaminated. To detect the former possibility a pressure gauge was permanently installed in each chamber, and to check on the latter the polonium alpha-particle pulses were periodically checked against the calibration voltage. As a further routine check the ionization chambers were occasionally interchanged, and also their individual counting rates for cosmic rays were intercompared. The photographic records, rather than simply the number of counts, have been used as the primary source of all our data. A microscope with a scale in the eyepiece was used to measure pulse heights; the calibration pulses were measured in the same way and a calibration curve drawn for each chamber and for each run.

2. Placement of Ionization Chambers: Arrangement A

The ionization chambers give four measurements of the particle density of each large shower which strikes in their vicinity. The principal object of the experiment was to obtain direct information on the structure of these showers, and two of the arrangements used were designed for this purpose.

The first series of experiments was carried out at Climax, Colorado, at 3500 meters, during the winter of 1946–7. "Arrangement A" in Fig. 3 shows the principal set-up used at Climax. The four chambers were horizontally placed on a line, 1 meter apart and with their axes perpendicular to that line. The shack which housed the experiment had walls and roof of wood, $1\frac{1}{2}$ g cm⁻² thick.

This arrangement was chosen because it was felt that such a "cross section" of the showers

which struck in the vicinity would show up the occurrence of multiple, spacially separated cores in the air showers.²⁰ One might expect to see an occasional event in which large pulses in the two extreme chambers were accompanied by smaller pulses in the middle chambers.

3. Arrangement B

A second type of experiment involves the statistical analysis of air showers and for this purpose it is necessary to study the air-shower-caused coincidences between two ionization chambers placed quite close together. The appropriate configuration is illustrated as "arrangement B" in Fig. 3. The four ionization chambers were arranged as two pairs, each pair consisting of one chamber directly above the other. Only the top chambers were used for quantitative analysis, but the criterion for a true air shower included the requirement that the bottom chambers show pulses. The necessity for this precaution was brought to light in the course of some other investigations which are reported in BHRW, reference 16. There it is shown that most of the bursts in an unshielded ionization chamber of the type used in these experiments are caused by nuclear disintegrations (heavily ionizing particles which are produced locally). For example, in one of our chambers at 3500 m, 98 percent of the bursts of more than 7.5 Mev are nuclear events; 2 percent are air showers. Cloud-chamber records of nuclear events²¹ show many in which some moderately high energy heavy particles are emitted, particles which are easily capable of penetrating the thin walls of our ionization chambers. The low probability that such an event will simultaneously cause large pulses in two ionization chambers proves to be offset by the enormously greater frequency of the nuclear disintegrations. Three and even four chambers may be affected this way, and it is only by using what amounts to four-chamber coincidence that one finally reduces the nuclear events to a negligible fraction of the showers.²²

²⁰ Such a possibility had been discussed in connection with the experiments of Lewis, reference 5, which did not show agreement with the cascade theory. Cf. M. M. Mills and R. F. Christy, *Phys. Rev.* **71**, 275 (1947).

²¹ W. Hazen, *Phys. Rev.* **63**, 213 (1943).

²² Clearly, a very high gas pressure in the chamber will eventually favor the detection of showers, and it turns out that requiring a very large energy loss has the same effect.

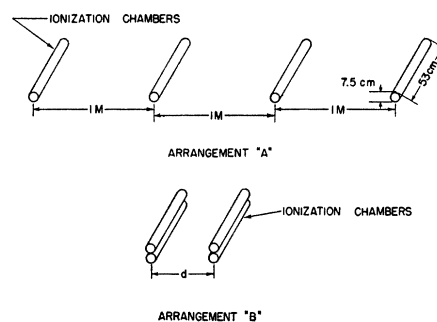


FIG. 3. Disposition of the cylindrical ionization chambers in arrangements A and B.

Arrangement B was used, with various distances separating the two pairs, at the second high altitude station, Doolittle Ranch (near Echo Lake), Colorado. There at an altitude of 3050 meters a series of experiments on air showers was carried out during the summer of 1947, with the assistance of R. Davisson. These experiments were done in the open, with only canvas over the ionization chamber containers.

Arrangement B was also used in Climax in connection with another experiment and with a bias different from that used in arrangement A, but within the rather large statistical error the results can be extrapolated to compare with those from arrangement A.

4. Arrangement C

Figure 4 shows arrangement C, which yields the most detailed description of the showers. Three chambers were placed at the corners of an equilateral triangle, 12.2 meters on a side, and the fourth was placed in the center. In addition, we were fortunate in having available for part of the time a cloud chamber operated by W. E. Hazen. This cloud chamber was being used for another study, but it was also tripped by a signal from our equipment whenever our addition circuit fired. Identification of the pictures was accomplished by photographing clocks on both cloud-chamber and ionization-chamber records. The cloud chamber was just outside the triangle, as shown in Fig. 4.

Arrangement C was used both at Doolittle

Thus Lapp (reference 6), whose ionization chamber had a pressure 10 times ours, and who required 100 times the energy loss, reported that about 85 percent of his bursts at sea level were caused by air showers.

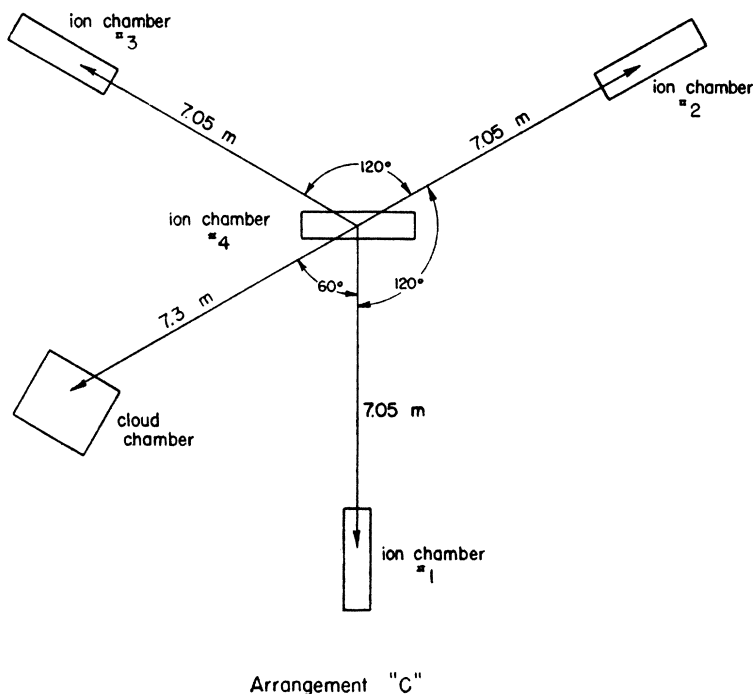


FIG. 4. Disposition of the cylindrical ionization chambers in arrangement C.

Ranch (3050 m) and at the top of Mt. Evans (4300 m).

IV. RESULTS

1. Qualitative Structure of Individual Showers

The principal objective of these experiments was to gain information on the structure of individual air showers, by finding the particle density at several points in each shower. An examination of the 250 showers which were recorded in arrangement *A*, during 240.5 hr. of operation, shows that they have the qualitative structure which is expected if they arise by cascade multiplication from a single electron or photon (i.e., particle density decreasing monotonically with distance from a unique core). In a great majority of the cases the pulses were all about the same size. All but seven of the showers gave measurable pulses (greater than $\frac{1}{8}$ the minimum pulse required for coincidence) in all four chambers. One had pulses in three adjacent chambers. Six had pulses only in an end chamber and its neighbor.

There were three records in which two non-adjacent chambers showed pulses. Since the expected number of such double accidentals from

alpha-particles was between one and two, these were assumed to be accidental coincidences. Obviously, some of the six double coincidences between adjacent chambers could also have been accidentals. Of the remaining 243 records, most of the groups are about uniform, many of them rising from one end of the group to the other, and some having a maximum. A few cases in which there was a minimum were not very pronounced, and undoubtedly could have been caused by fluctuations. There were a few cases in which the maximum was quite pronounced—as it should be if the shower struck nearby—and no cases of an equally pronounced minimum.

The three cases in which the singularity in the electron density function (see below) is best illustrated are described in Table I.

It should be noted that the "size" of an air shower does not have a precise meaning. Although a shower with very many particles will be detected over a large area, the particle density will nevertheless change violently over a distance of less than a meter in the vicinity of the shower core. Thus the small spacing used in arrangement *A* is already large enough to show the most characteristic feature of the shower structure, and, conversely, it is nearly impossible to make an

apparatus so small that the particle density incident upon it is always uniform.

Examination of the 540 showers registered during 325 hours of observation in arrangement *C* at 3050 meters leads to the same general conclusion: the structure of these showers seems normal. Often the center chamber will have a larger pulse than its neighbors, or there will be a gradual increase in pulse height from one side to the other. In no case is the central chamber significantly smaller than all its neighbors. The quantitative analysis of the Arrangement *C* data will be described below.

The regularity of these results also leads to the observation that the probability for an air shower to cause a nuclear disintegration in an ionization chamber must be very small. This result would follow from the evidence, presented in BHRW, that most nuclear disintegrations are not caused by photons.

2. Coincidence Rate as Function of Separation between Chambers

Statistical analysis of air showers can be based on the coincidence rate between two ionization chambers as a function of their horizontal distance of separation. (Auger calls the analogous function for Geiger tubes a "decoherence curve.") All of the experimental arrangements which have been described yield information on this function; it will be represented here by $W(\rho, d)$ = number of coincidences per hour between two ionization chambers separated by distance d meters and each required to have a particle density $\geq \rho$ particles per square meter. Arrangement *B* yields this function directly; at each distance of separation one simply adds up, by inspecting the record of pulse heights, the number of times the two top chambers simultaneously had pulses corresponding to particle density $\geq \rho$, for various values of ρ . The dependence of W on ρ which is found in this way can be represented, within the statistical error, by a power law, $W = \text{constant} \times \rho^{-\gamma}$, and both the constant and the exponent prove to be functions of the distance d . A similar examination of arrangement *A* in which one concentrates on only two chambers, ignoring what happens in the other two, gives W for three values of d ; Arrangement *C* gives W

TABLE I. Three showers which struck near the apparatus, arrangement *A*. The numbers represent probable values for the number of electrons which went through the chamber.

Chamber 1	Chamber 2	Chamber 3	Chamber 4
200	204	61	32
10	5	40	135
15	119	15	21

for two values of d (the side of the triangle and the distance from a vertex to the center).

Table II summarizes the data on the function W . In analyzing the data at 3050 meters and 4300 meters a minimum particle density of 460 particles/m² was chosen, although records were available down to a particle density of 308 particles/m². In this way the discrimination is entirely done by the photographic record; if one chose the minimum to correspond to that of the electrical selection (308 particles/m²), the selection of showers would rest partly on electrical discrimination and partly on the photographic record.

The second column shows the actual number of showers observed with the minimum ρ selected. The fourth column shows the best value of γ , the exponent in the density law, obtained from the data at that particular distance. Thus the function W for 0.15 m at 3050-m elevation, for example, can be written

$$W(\rho, 0.15) = 0.99(460/\rho)^{1.50} \text{ coincidences/hour}$$

in the range $300 < \rho < 2000$ particles/m².

TABLE II. Coincidence vs. distance data.

3050 Meters			
Distance	No. of coins. with 460 part/m ²	Coins. per hour	γ
0.15 m	58	0.99	1.50
0.36 m	96	1.04	1.67
1.00 m	47	1.09	1.56
7.05 m	134	0.51	1.85
12.20 m	109	0.42	1.90
3500 Meters			
Distance	No. of coins. with 615 part/m ²	Coins. per hour	γ
0.23 m	37	1.22	Average value of γ is 1.7
1.00 m	89	0.70	
2.00 m	83	0.65	
3.00 m	72	0.57	
4300 Meters			
Distance	No. of coins. with 460 part/m ²	Coins. per hour	γ
7.05 m	103	1.60	1.8
12.20 m	75	1.16	2.2

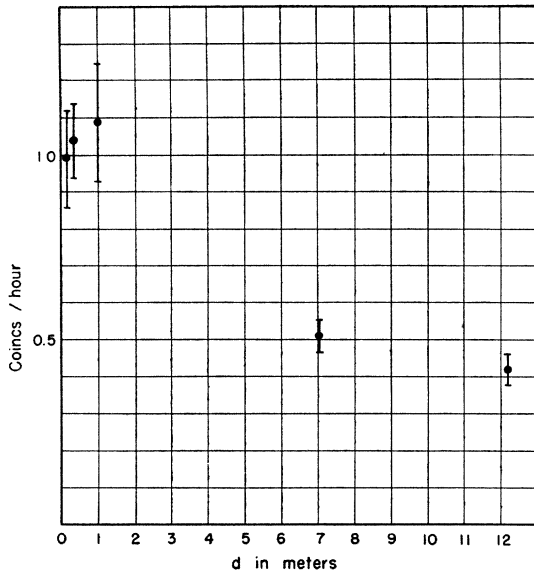


FIG. 5. The coincidence rate vs. separation of ionization chambers for 3050 m.

At 3050 m the data for $d=0.15$ m, 0.36 m, and 1.0 m were obtained with arrangement B. The data for $d=7.05$ m and 12.2 m were obtained from arrangement C both at 3050 m and 4300 m. At 3500 m the data for $d=0.23$ m were obtained with arrangement B, the rest with arrangement A. The statistics did not seem to warrant obtaining separate values of γ for each distance. It should be noticed that the minimum value of ρ is different here, so that the counting rates are not directly comparable with those at 3050 m. The 3500-m data should be multiplied by about $(615/460)^{1.7} = 1.63$ to compare with the other.

The decoherence curves from the low altitude data in Table II are shown in Figs. 5 (3050 m) and 6 (3500 m). The agreement between the two sets of data is not perfect, owing mainly to the 0.23-m point on the latter curve, which has a very large error. As previously explained, this point is obtained from another experiment, and its error involves the value of γ as well as the statistics from number of counts. We will use the more complete and accurate curves of Fig. 5 in analyzing these results.

The Geiger-tube experiments of Cocconi and co-workers also yielded an air shower rate as function of particle density. At 2200 m, using a triangular arrangement four meters on a side, they found a rate $W = 3600(1/\rho)^{1.55} \text{ hr.}^{-1}$, where ρ

is an average particle density over the apparatus; the range of ρ was 10 to 220 particles/m². When the altitude difference is corrected this should be approximately comparable with our interpolated rate at four meter separation, Fig. 5, even though the arrangements are not identical. Choosing a particle density intermediate between the two experiments we find that, for the same rate, they measure a density 11 percent lower than ours, which is quite satisfactory agreement.

From Table II it appears that γ increases with distance. γ is obtained as the slope of the best straight line drawn through the graph of $\log W$ against $\log \rho$ at a particular distance. Since the points on such a graph are not independent, it is hard to decide what the reasonable limits of error on γ might be. In order to see whether or not the change in γ is real, we have plotted the differential frequency curves for the two extreme distances. These curves yield values of $\gamma+1$, and the error of each point is independent. $\log(\Delta W/\Delta \rho)$ is plotted against $\log \rho$, for $d=0.15$ m and $d=12.2$ m, in Figs. 7 and 8, with the statistical errors indicated. ρ is indicated in arbitrary units. Since the number of cases is not great,

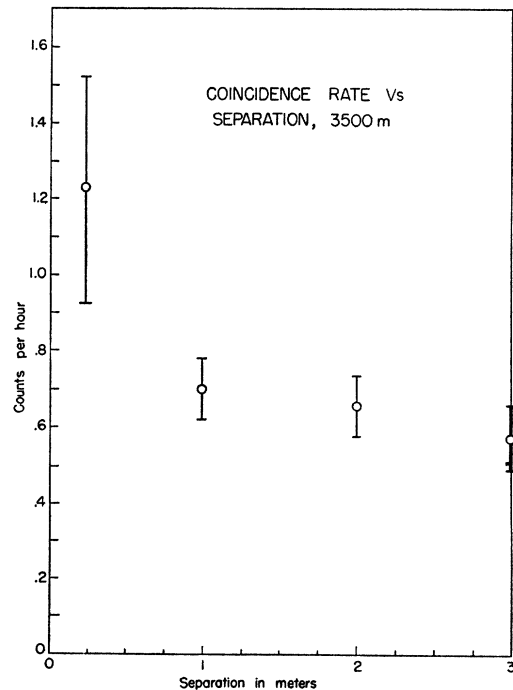


FIG. 6. The coincidence rate vs. separation of ionization chambers for 3500 m.

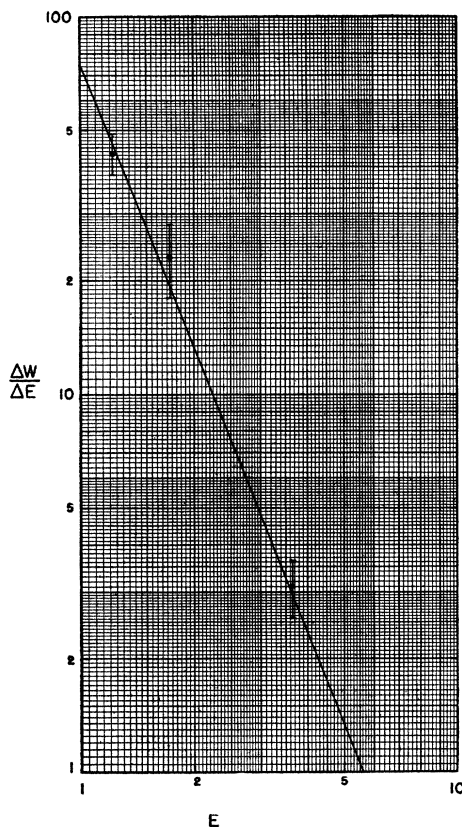


FIG. 7. Differential distribution curve of number of coincidences as function of particle density, at 0.15 m separation. E is the particle density in arbitrary units.

only three ranges of $\Delta\rho$ are taken, and the approximately correct abscissas are found by assuming the value of γ which the integral curve gives in each case. The extreme values of $\gamma+1$ which can be obtained from these curves by drawing lines which are just within the errors are at 0.15 m: 2.14 and 2.70; at 12.2 m: 2.75 and 3.14. The lines drawn on the graphs correspond to the assumed values of γ derived from the integral curves. The increase of γ with distance seems to be real.

3. Angular Distribution

During some of the runs at 3050 m, the cloud chamber was operating and was tripped every time a shower struck the apparatus with a particle density greater than 308 particles/m² in the vicinity of at least two ionization chambers. It turns out that this does not always represent a high enough particle density near the cloud

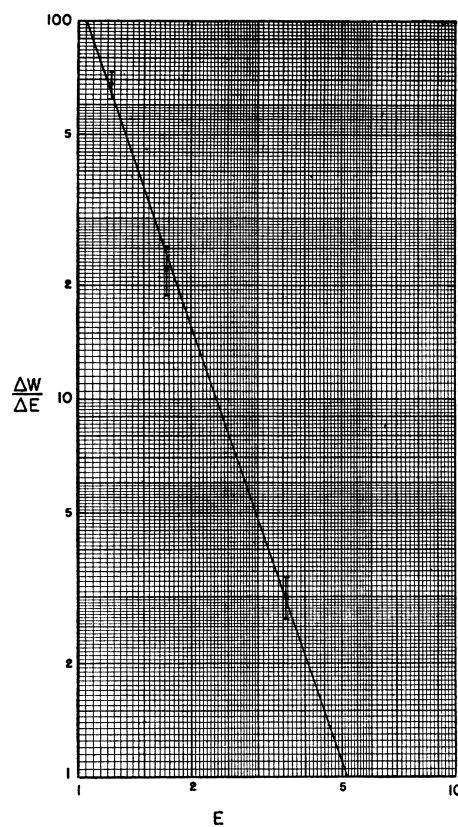


FIG. 8. Differential distribution curve at 12.2-m separation.

chamber to make the shower show up clearly. If the shower struck near chamber 2, for example, its density near the cloud chamber might be quite small. Also the scattering of low energy electrons tends to reduce the number of tracks which show a coherent direction. A certain discrimination in favor of large showers therefore operates, since about 30 percent of the pictures have to be rejected.

Figure 9 shows the resulting distribution of air showers as function of projected angle, using all available photographs. (The projected angle is the angle one sees on the photographic film, and of course is always less than or equal to the true zenith angle in space.) If α is the projected angle, θ the zenith angle, and ϕ the azimuthal angle, $\tan\alpha = \tan\theta \cos\phi$. A consequence of this is that if the distribution per unit solid angle in space is of the form $\cos^m\theta d\Omega$, the distribution in projected angle is of the form $\cos^m\alpha d\alpha$.²³ Thus the

²³ J. Daudin, *J. de Phys. et rad.* **7**, 302 (1945).

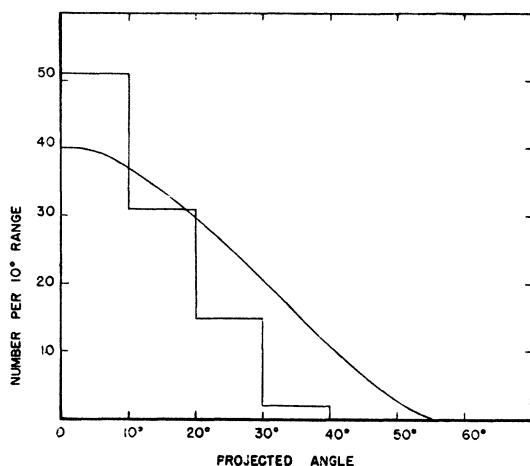


FIG. 9. The distribution in projected angle of large air showers at 3050 m. Smooth curve is the calculated distribution, arbitrary normalized.

sharp maximum of Fig. 9 shows that most of the showers at 3050 m are almost vertical. This is in fair agreement with a similar study of Daudin,²³ though he seems to find a slightly flatter distribution, perhaps because of having selected larger showers.

We use the observation that most showers are vertical to simplify the analysis of the local behavior of air showers. For example, the fact that nearly all showers have $\theta < 30^\circ$ means that the uncertainty in apparent distance between two ionization chambers is <13 percent. One can show that this causes only a very small change in the shape of the decoherence curve.

The angular distribution will be compared with theoretical predictions in Section V-6.

V. ANALYSIS

1. Application of Cascade Theory

Since the large air showers have the qualitative appearance of cascades, we will try to apply some results of the cascade theory to the data. In the first approximation the cascade theory^{11,17} treats all particles as though they traveled along the same straight line, and yields, for example, the spectrum of electrons in the shower as it reaches thickness t , having started at $t=0$ with a single electron of energy E_0 . If energies are measured in terms of the "critical energy" ϵ and thickness is measured in terms of the "radiation length" X_0 , the results of cascade theory can be ex-

pressed independent of the material. X_0 and ϵ are defined in reference 17, but it has been pointed out²⁴ that the contribution of the atomic electrons to pair production and radiation cross sections must be considered. This lowers the values given in reference 17; we have used $\epsilon = 86$ Mev, $X_0 = 36$ g cm⁻² for air.

The lateral spread of the cascade electrons (which is essential for the interpretation of experiments on air showers) arises almost entirely from multiple Coulomb scattering. Most of the calculations of the lateral distribution function refer only to the point of maximum development of the shower. In many experiments the showers recorded are mostly near their maximum, and Moliere¹¹ argues that it is a reasonable approximation to assume that all observed showers have the same lateral distribution function. In the experiments reported here the smallest showers we record must be well past the maximum; nevertheless we will use this assumption, i.e., that all showers are geometrically similar, and are similar to themselves over their whole length.

The particle density at a depth t below the top of the atmosphere, and distance r' from the

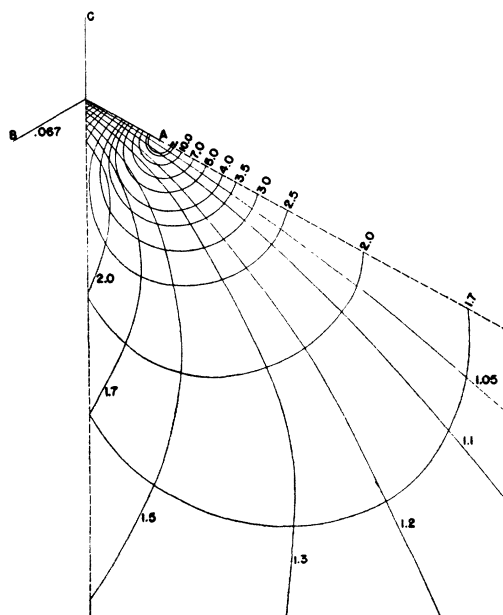


FIG. 10. Chart for the location of the center of individual showers. Each line corresponds to the ratio of particle densities indicated.

²⁴ J. A. Wheeler and W. E. Lamb, Jr., Phys. Rev. 55, 858 (1939).

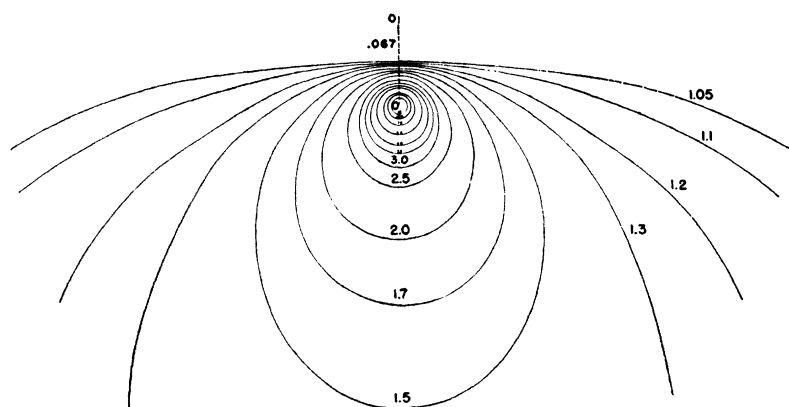


FIG. 11. The second chart for the location of individual showers. Reading from the center circle the numbers are 15, 10.0, 7.0, 5.0, 4.0, and 3.5.

axis of the shower, can then be expressed as $\rho = N(t)f(r')$, where $N(t)$ is the total number of electrons at depth t , and $f(r')$ is the function calculated by Moliere.¹¹ r' must be measured in units of the "characteristic scattering length"

$$r_1 = (X_0/\epsilon)E_s.$$

E_s is 21 Mev¹⁷, so that $r_1 = 74$ m at sea level, 106 m at our 3050-m station. For $f(r')$ we use the analytic approximation given by Bethe,²⁵

$$f(r') = \frac{0.454}{r'}(1 + 4r')\exp[-4(r')^2]. \quad (1)$$

2. Analysis of Individual Showers: Theory

Knowledge of the particle density at four points in a shower should enable one to compute the location of the axis of the shower if a lateral density distribution function is assumed. The linear disposition of arrangement *A* proved unsatisfactory for this purpose, both for geometrical reasons and because the distance between ionization chambers was too small. The triangular form and larger spacing of arrangement *C* were therefore adopted to make this direct test of the shower structure.

The four ionization chambers give four simultaneous measurements of the particle density $\rho(r') = Nf(r')$, where r' is the distance of the ionization chamber from the axis of the shower and $f(r')$ is the structure function, which we assume to be that calculated by Moliere, Eq. (1). Any two measurements of ρ determine a line which the axis must intersect as it crosses the

plane of observation; four measurements therefore determine three lines, which should meet in one point if $f(r')$ is correct.

Figure 10 is a small-scale reproduction of a chart of these lines of constant ratio of density for the ratios between the points labeled *A* and *C* (the lines circling point *A*) and between *B* and *C* (circling point *B*). The charts were prepared with the help of the Laboratory's Computing Group, using the form of the Moliere function given in Eq. (1). The scale is determined by the distance from the center to any one of the chambers *A*, *B*, or *C*, as this must correspond to the actual distance in arrangement *C*, or 7.05 m/106 m = 0.067 characteristic scattering lengths at 3050 m. The numbers on the lines are the density ratios. Figure 11 is a similar chart, but with the distance between the two chambers equal to 0.067. It therefore corresponds to the central ionization chamber and any one of the three outside ones. (The central chamber is referred to as "0.")

To locate a shower, one reduces the four pulse heights to particle densities by means of the calibration. Chambers 1, 2, and 3 are the outside chambers; the chamber with the largest particle density is made to correspond to *A*, the next to *B*, the smallest to *C*. Then the ratio *A/C* places the shower axis on one of the lines encircling *A*, *B/C* places it on one of the other lines, and in general the two lines will intersect in two points, one inside the circle circumscribing *ABC* and one outside. Because of the order of *A*, *B*, and *C*, only one sextant of the chart is used. The ratio *A/C* or *C/A*, whichever is larger, places the shower axis on one of the lines in the original of Fig. 11,

²⁵ H. Bethe, Phys. Rev. 72, 172 (1947).

TABLE III. Location and energy measurements on individual showers.

A/C	B/C	A/O	O/A	N_1 $\times 10^{-6}$	N_2 $\times 10^{-6}$	N_3 $\times 10^{-6}$	N_4 $\times 10^{-6}$	N_{Av} $\times 10^{-6}$
1.5	1.05		1.6	2.5	1.8	1.6	1.5	1.9
1.7	1.25		>3.0	2.4	2.5	2.4	>2.3	2.4
1.4	1.05		2.0	1.9	3.4	2.6	2.2	2.5
2.6	1.95		2.15	2.8	2.5	3.1	3.3	2.9
1.8	1.6		2.05	3.2	3.4	3.1	3.1	3.2
2.8	1.8	1.0		4.2	3.4	3.9	3.4	3.7
4.0	1.3	3.3		5.7	4.9	4.1	3.6	4.6
1.6	1.5	>1.9		4.7	4.6	4.6	>2.5	4.6
>3.7	1.15	>1.83		5.2		5.2	5.2	5.2
4.5	2.2	1.5		5.5	4.5	5.5	5.7	5.3
4.0	1.2	2.9		5.8	7.0	6.6	5.7	6.3
3.4	1.45	3.3		7.3	7.7	7.1	4.5	6.7
4.8	1.34	2.45		6.7	6.6	6.9	7.1	6.8
3.8	1.25	2.7		6.8	7.0	7.3	5.9	6.8
>2.7	2.25	>1.0		7.5	>6.5	6.8	7.3	7.2
1.8	1.8	1.85		10.0	8.1	9.9	5.8	7.9
2.8	1.1	1.6		7.8	7.9	7.4	9.1	8.1
1.8	1.8	1.9		8.7	8.5	9.7	5.6	8.1
1.9	1.4	1.9		8.5	10.0	8.5	6.5	8.4
2.7	2.4	1.9		9.8	9.6	8.5	6.6	8.6
2.2	2.0	1.55		9.4	9.7	9.7	8.0	9.2
3.0	1.15	2.1		9.7	9.8	9.8	9.5	9.7
>3.0	1.5	>2.0			9.8	9.8	9.8	9.8
>2.5	1.0	>1.6		>4.6	11.0	10.0	9.5	10.2
2.1	1.8	1.1		12.0	12.0	12.0	14.5	12.6
2.6	1.2	1.9		13.0	13.0	13.0	12.0	12.8
2.85	1.0	1.6		12.0	12.0	13.0	16.5	13.4
1.65	1.3	1.65		19.0	16.0	15.0	13.0	15.8
>2.0	1.73	>1.25		16.0	16.0	>11.0	16.0	16.0
>2.2	1.4	>1.3		16.0	16.0		16.0	16.0
2.5	1.0	1.8		16.0	17.0	16.0	16.0	16.3
3.1	1.4	1.5		21.0	16.0	19.0	21.5	19.4
2.5	1.0	2.1		25.0	25.0	>27.0	22.0	24.0
2.1	1.05	2.1		26.0	26.0	29.0	21.0	25.5
1.7	1.1	1.3		26.0	26.0	25.0	27.0	26.0
2.0	1.05	1.3		30.0	30.0	30.0	36.0	31.5
>1.6	1.1	>1.35		93.0	103.0	103.0	98.0	101.3
1.4	1.0		1.18	Shower struck too far away to be measured				
1.1	1.4	1.3		Shower struck too far away to be measured				
1.55	1.2	1.75		Shower struck too far away to be measured				
1.6	1.2	1.25		Shower struck too far away to be measured				
1.4	1.15	1.3		Shower struck too far away to be measured				
1.2	1.1	1.2		Shower struck too far away to be measured				

plus four (4) showers too large to be measured.

which is drawn on tracing paper and can be superposed on the chart of Fig. 10. If the theory is correct, this line should pass through one of the two points of intersection of the two lines already chosen.

The other ratios (e.g., center to *B*) are not independent and therefore add no new information.

If it were possible to determine the particle densities accurately this method would be a sensitive test of the Moliere theory, because it is not likely that another type of shower would fit (notice that even with only three chambers not all data would fit these curves—the ratio *B/C* cannot be greater than 2.4). However, the statistics of individual particle density measurements are poor, since the sample taken from the shower is small.

When *n* uniformly ionizing particles from a Poisson distribution cross a cylindrical ionization chamber of our type perpendicular to the axis, the fractional error in the density measurement

is greater than $n^{-1/2}$ because the particles near the axis contribute more to the total ionization than do the particles near the edge. If all the ionization is collected, the error is $1.76n^{-1/2}$. However, electron collection favors the particles which pass near the edge (cf. BHRW), so that the error is smaller, and we take $1.5n^{-1/2}$ for our error estimates. For most of the showers in arrangement *C* the particle density in at least one chamber was so low that the data could not be subjected to this detailed analysis. Only those showers were chosen for analysis, therefore, in which all four chambers had particle densities corresponding to at least 616 particles/m², or 24 particles per chamber. The maximum fractional error is then $1.5/(24)^{1/2} = 0.31$, and in the worst case (equal minimum particle densities) the error in a ratio of particle densities is $0.31 \times \sqrt{2} = 0.44$.

3. Analysis of Individual Showers: Results

During the 325 hours of observation in arrangement *C*, 47 showers were recorded which satisfied the minimum pulse height criterion established above. The analysis of these 47 showers is given in Table III. The ratios *A/C*, *B/C*, etc., have been explained above. For each shower we have found the best location of the shower axis, and measured the distance from this center to each chamber. Since the pulse size in chamber 1 gives ρ , and the shower location gives r' , we know the total number of particles in the shower at the plane of observation: $N = \rho(r')/f(r')$. The next columns give the values of *N* corresponding to each chamber, and the last column is the average of the four.

The agreement between the different values of *N* for the same shower furnishes a measure of the agreement of these data with the hypothesis that these showers are simple cascades. Table III shows that the fluctuations of *N* are within the statistical error, and therefore that these showers agree with this hypothesis.

Occasionally the shower struck so near one ionization chamber that its amplifier was saturated. These cases are distinguishable by a > sign before one or more ratios. For the three cases of this type for which a blank appears in an *N* column the shower center was not over-determined.

The six showers at the end of the table are all consistent, within the statistical error, with axes which struck too far from the apparatus to be located (more than 40 m). Four showers saturated more than one ionization chamber and therefore could not be analyzed.

4. Statistical Results: The Shower Rate

In order to interpret statistical results such as the decoherence curve it is necessary to assume some spectrum (i.e., frequency distribution) of cascade showers. Often one takes a spectrum of primary electrons at the top of the atmosphere, but it is sufficient merely to assume a local distribution of showers at the altitude of the observations. Thus, we let $S(N, t)$ be the number of showers, per square meter per hour, which contain more than N electrons as they cross the depth t ; N is the number of electrons which cross a horizontal plane at depth t , in a given shower. (Recall that we are now assuming all showers to be vertical.) This function S is a convenient way to join experiment (which can determine S directly, in principle at least) with a theory of the origin of the showers (which must account, for example, for the variation of S with t).

The decoherence curve function $W(\rho, d)$ is given by an integral over $S(N)$. The observed power-law dependence of W on ρ suggests a power-law form for $S(N)$. Blatt²⁶ has made a detailed analysis of the decoherence curve for power-law $S(N)$, assuming Moliere's structure function $f(r')$. Agreement of the theory with the experimental points of Fig. 5 is not very satisfactory, and the probable cause of the discrepancy is discussed in Blatt's paper. It appears that the theory is more likely to be correct at the larger separation distances, and we therefore use the points at 7 m and at 12.2 m to obtain the absolute shower rate. From Blatt's analysis, the number of showers per square meter per hour, of more than N particles, at 3050-m elevation, is $S = 1.8 \times 10^{-3} (N/10^6)^{-1.5} \text{ m}^{-2} \text{ hr}^{-1}$, $10^5 < N < 10^6$, $S = 1.8 \times 10^{-3} (N/10^6)^{-1.9} \text{ m}^{-2} \text{ hr}^{-1}$, $10^6 < N < 10^8$. It should be emphasized that the absolute value of this result depends on the assumption that Moliere's structure function applies to all showers.

In Section 3 we have shown that the results of measurements on individual showers agree with the Moliere function. However, the showers which could be analyzed in this way were all large, and therefore fairly near their maximum. Many of the showers which contribute to the decoherence curve of Fig. 5 are much smaller, and presumably well past their maximum. Also the absolute value of S depends on the normalization of the structure function. Since this function was tested only for distance $r < 0.4r_1$, one cannot conclude that the normalization is correct. Therefore the value which we give for S is uncertain, perhaps by as much as a factor of two.

5. Altitude Variation: Assumptions about the Primaries

The data in Table II have been used to infer a local shower spectrum $S(N)$, at 3050 m. The data at 4300 m are less complete, but if we assume the same form of $S(N)$, we can find the factor relating the number of showers per square meter per hour at this altitude to that at 3050 m. This proves to be $S(N, 4300)/S(N, 3050) = 3.6 \pm 0.4$. The range of N which contributes most to this result is about $10^5 - 10^7$ particles, corresponding to the minimum accepted particle density of 460 particles/m².

This result can be used to test theories of the origin of large air showers, since these theories may predict different altitude dependences. The altitude dependence is also sensitive to the form of the production spectrum, i.e., to the exponent if a power law is assumed, but the value of this is circumscribed by the experimentally determined form of $S(N)$.

If we assume a primary electron spectrum, letting $F(E_0)$ be the number of electrons per square meter per hour per steradian in the vertical direction, then at depth t ,

$$S(N, t) = F[E_0(N, t)],$$

where, if Π is the total number of electrons as defined in Rossi and Greisen, $N = \Pi(E_0, 0, t)$. If we assume that the shower-initiating electrons are secondaries, produced in the atmosphere with a mean free path λ ,

$$S(N, t) = \int_0^t F[E_0(N, t - \tau)] e^{-\tau/\lambda} (d\tau/\lambda).$$

²⁶ J. M. Blatt, Phys. Rev., in print.

TABLE IV. The number of showers of more than N particles, $S(N)$, per square meter per hour per steradian, in vertical direction, calculated for various assumptions about the primary. Depth measured in radiation lengths.

Assumptions about primary	Atmospheric depth	$S(10^4)$	$S(10^5)$	$S(10^6)$	$S(10^7)$
Electrons $\gamma=1.8$	16.8	3.14×10^{-2}	8.52×10^{-4}	1.63×10^{-5}	2.34×10^{-7}
	28.6	8.20×10^{-4}	5.30×10^{-5}	2.61×10^{-6}	3.73×10^{-8}
Electrons $\gamma=2.0$	16.8	6.98×10^{-2}	1.27×10^{-3}	1.57×10^{-5}	1.40×10^{-7}
	28.6	1.22×10^{-2}	5.81×10^{-5}	2.06×10^{-6}	1.84×10^{-8}
Single production $\lambda=100 \text{ g cm}^{-2}$ $\gamma=1.8$	16.8	6.31×10^{-2}	1.07×10^{-3}	1.44×10^{-5}	1.45×10^{-7}
	28.6	1.07×10^{-2}	1.04×10^{-4}	3.80×10^{-6}	8.78×10^{-8}
Multiple production $\lambda=0$ $\gamma=1.8$	16.8	4.10×10^{-3}	1.83×10^{-4}	6.32×10^{-6}	1.34×10^{-7}
	28.6	2.50×10^{-5}	1.48×10^{-5}	7.50×10^{-6}	3.09×10^{-9}
Multiple production $\lambda=200 \text{ g cm}^{-2}$ $\gamma=1.8$	16.8	3.63×10^{-2}	7.26×10^{-4}	1.39×10^{-5}	2.12×10^{-7}
	28.6	4.60×10^{-3}	1.00×10^{-4}	2.13×10^{-6}	3.86×10^{-8}

Recently the possibility has been pointed out²⁷ that the high energy soft component may arise from decay of neutral mesons produced in a highly multiple process. According to this theory, a primary proton of energy E_0 would lose a large fraction of its energy in a single act of meson production, producing on the average about $\nu = 2(E_0/\mu)^{\frac{1}{2}}$ mesons, where μ is the meson mass. This would lead to an air shower started by $\sim \nu/3$ neutral mesons (decaying quickly into gamma-rays) with average energy E_0/ν . We have made an estimate of the S arising from this case, using slightly different numerical coefficients (the calculation was done before the detailed results of reference 27 were available). We assumed that $\nu = (E_0/10^8)^{\frac{1}{2}}$, that all mesons have energy E_0/ν , and that all mesons give rise to showers. Then E_0 is related to N and t by $N = \nu \Pi(E_0/\nu, 0, t)$, and the calculation of S goes through as before.

TABLE V. Calculated ratio of the number of showers per square meter per hour, of more than N particles, between 4300 meters and 3050 meters, for various values of N and various assumptions about the primary.

N	Primary electrons, $\gamma=1.8$	Primary electrons, $\gamma=2.0$	Single production, $\lambda=100 \text{ g cm}^{-2}$ $\gamma=1.8$	Multiple production, $\lambda=200 \text{ g cm}^{-2}$ $\gamma=1.8$
10^4	$\frac{S(4300)}{S(3050)} = 2.94$	3.20	1.82	1.78
10^5	2.40	2.50	1.94	1.79
10^6	1.74	1.86	1.51	1.86
10^7	1.62	1.67	1.28	1.69

²⁷ H. W. Lewis, J. R. Oppenheimer, and S. A. Wouthuysen, Phys. Rev. **73**, 127 (1948).

Values of S for these possibilities have been calculated numerically assuming power-law production spectra. The production spectrum is normalized in all cases to the number of "primary" particles of greater than 10^{15} ev according to the Heisenberg-Euler spectrum,²⁸ 2.2×10^{-4} particles $\text{m}^{-2} \text{hr}^{-1} \text{sterad}^{-1}$. The assumed production spectrum therefore becomes $2.2 \times 10^{-4} (10^{15} \text{ ev}/E_0)^\gamma \text{m}^{-2} \text{hr}^{-1} \text{sterad}^{-1}$. Table IV shows some values of S for various values of the parameters.

To compare with the observed values of ionization chamber counting rates, we must integrate over all angles. A single ionization chamber²⁹ is non-directional, so that we want

$$S_1(N, t) = \int_0^{\pi/2} S(N, t/\cos\theta) 2\pi \sin\theta d\theta =$$

the number of showers crossing a sphere of unit cross section. This function should compare directly with the S derived from the decoherence curve.

Ideally one should adjust the assumed production spectrum until the calculated S_1 has the same form as the observed S . However, the power-law spectra assumed here prove to match the observed form of S fairly well. For primary electrons, a spectrum of power 1.9 would seem to match the data best.

Table V gives the calculated altitude variations of S for several cases.

6. Angular Dependence

The angular dependence of the large air showers can be calculated by a method similar to that for the altitude variation. The results are less accurate because it is necessary to calculate the counting rate of an ionization chamber using the number of showers coming in a particular direction, $S(N, t/\cos\theta)$. With a power-law primary, this function does not approximate a power law in N so closely as S_1 does.

The calculated distribution in projected angle, for primary electrons with $\gamma=1.8$, is shown as the solid curve in Fig. 9.

²⁸ W. Heisenberg, *Cosmic Radiation*, ed. by W. Heisenberg (Dover Publications, New York, 1946), Ch. 1.

²⁹ The effect of finite separation between two chambers makes the calculation very complicated. An estimate shows that the method used here is sufficiently accurate for the altitudes used in these experiments.

VI. DISCUSSION

1. The Measurements on Individual Showers

In Section V the cascade theory was applied to the detailed results obtained on individual air showers, and it was seen that within the limited statistical accuracy the results were consistent with the theory. Assuming the validity of cascade theory it is possible to find the total energies of the events tabulated in Table III. The number of particles in the showers at the plane of observation, 20 radiation lengths below the top of the atmosphere, ranges from 2×10^6 to 10^8 . Figure 12 shows the necessary primary energy for an electron which creates N electrons at the maximum development of its shower. For $N = 10^7$ it is $1.4 \times 10^8 \times \epsilon = 1.2 \times 10^{16}$ ev. There seems to be ample evidence for primary particles of 4×10^{16} ev and perhaps even 10^{17} ev.³⁰

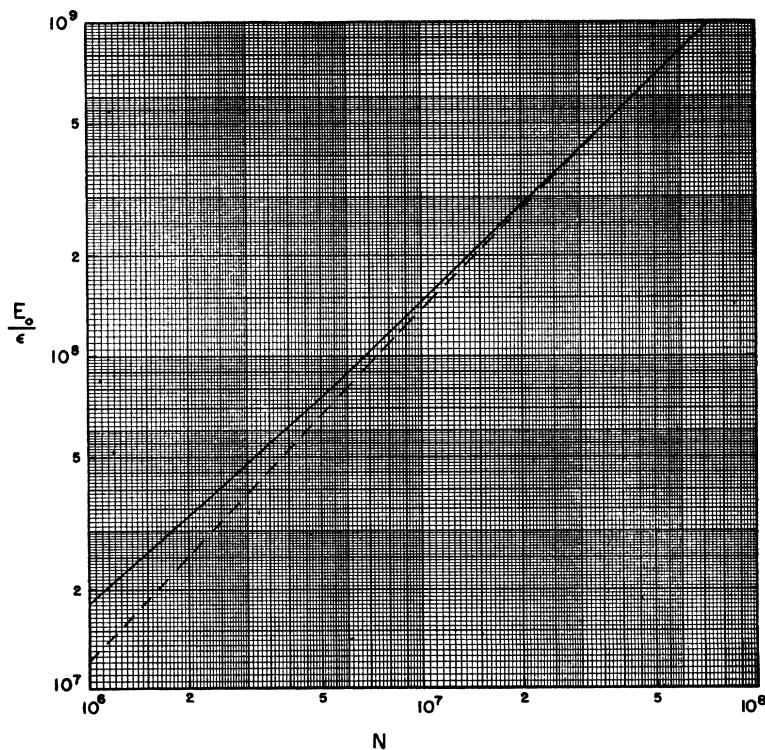
The values for N in Table III depend on the normalization of the Moliere structure function, of course. The dotted curve in Fig. 12 gives the

minimum energy corresponding to a given N ; if the initial electrons were produced in a multiple process, this curve still represents the minimum energy which could have initiated the shower.

The measurements on individual showers are consistent with the Moliere distribution and therefore with the hypothesis that the primary particle is an electron or photon. Evidence has recently been obtained³¹ that not more than a few percent of the primary cosmic rays are electrons or photons. Also, production of cascade showers in lead by penetrating particles has been observed at high altitudes.³² Of course, the particles which cause the effects we observe constitute $\sim 10^{-9}$ of the primary cosmic rays, and are in a completely different energy range, but it is of some interest to inquire whether the process observed by Bridge, Hazen, and Rossi could also account for the large air showers.

It is clear that the structure of the air shower should be unchanged if it originates from a single electron or photon. If a large number of electrons

FIG. 12. Energy (in critical energy units) of initiating electron vs. number of electrons created: (a) after 20 radiation units (upper curve); (b) at shower maximum (lower curve).



³⁰ The effect which we observe could arise from a large group of particles, each with a much lower energy, but these particles would have to arrive at the earth in a bunch not more than 1 m across and 1000 m long.

³¹ R. I. Hulsizer and B. Rossi, Phys. Rev. **73**, 1402 (1948).

³² H. Bridge, W. E. Hazen, and B. Rossi, Phys. Rev. **73**, 179 (1948).

TABLE VI. Results expected from multiple meson production theory (assuming that showers start 100 g cm^{-2} below top of atmosphere). θl is the radius of the circle within which most cores will strike.

E_0	Multiplicity	$\theta_{r.m.s.}$	θl	Av. dist. between cores	Energy per core
10^{13} ev	46	1.4×10^{-2}	220.0 m	50.0 m	2×10^{11} ev
10^{14} ev	100	4.5×10^{-3}	72.0 m	13.0 m	10^{12} ev
10^{15} ev	200	1.4×10^{-3}	22.0 m	2.8 m	5×10^{12} ev
10^{16} ev	460	4.5×10^{-4}	7.2 m	0.6 m	2×10^{13} ev
10^{17} ev	1000	1.4×10^{-4}	2.2 m	0.12 m	10^{14} ev

were produced with average angles of emission similar to that encountered in pair creation ($\sim mc^2/E$), they would start showers whose cores would be separated by less than a centimeter when they reached our apparatus.³³ Because of the similarity principle of cascade structure, such an event could not be distinguished from a single cascade. If, however, a large number of electrons were produced in a single event of the type discussed by Lewis, Oppenheimer, and Wouthuysen,²⁷ it has been proposed that the electrons would be ejected with spherical symmetry in the center of gravity system. In this case they would have a rather large spread in the laboratory system, approximately Gaussian with the angle of standard deviation being given by $\theta_{r.m.s.} \sim 4(10^8 \text{ ev}/E_0)^{1/2}$. Table VI shows some numerical values for θ , for the expected multiplicity according to Lewis *et al.* (order of magnitude), for the radius θl within which most of the showers would hit at 20 radiation lengths³⁴ below the top of the atmosphere, for the average distance between cores, and for the average energy per core.

It is seen that a unique core of the shower is no longer to be expected, with reference to the dimensions of our apparatus. If the cores are sufficiently spread out so that only one strikes near the apparatus, its energy is too low to be recorded. For showers of 10^{16} ev the cores are spread out over an area the size of arrangement C, and the results of arrangement A and arrangement C become unintelligible. A large number of separate cores, each contributing a particle density varying approximately as $1/r$,

³³ If one assumed an angle $\mu c^2/E$, where μ is the meson mass and E the meson energy, the separation becomes a few tens of centimeters for the showers of lowest energy.

³⁴ l , the distance from the point of creation of the shower, is 13,000 m if production takes place 100 g cm^{-2} below the top of the atmosphere.

lead to a much more uniform distribution in pulse heights than that expected from a single core. Thus even a shower whose "center" lies within the triangle of arrangement C will either be inconsistent with the Moliere distribution or will appear to have struck very far away. This qualitative observation has been verified by computing the pulse height distribution which would result from a number of assumed distributions of cores.

Examination of Table III shows that many of the showers exhibit a pronounced single-core structure. Nine of the showers in Table III struck inside the triangle of ionization chambers. The cases from arrangement A, in Table I, are equally striking. Because of the finite size of the ionization chambers the maximum ratio obtainable between two chambers 1 m apart is about 6, when the core strikes one chamber. This ratio is lowered if other cores strike in the vicinity of the two chambers, of course. Thus Table I can be understood only in terms of a single core. This core would have to correspond to an initial energy of about 10^{14} ev, and reference to Table VI shows the inconsistency: either we must assume all cores to be separated by many meters, in which case the energy of a *single core* is far too low, or we must assume that they all fall within a circle a few tens of centimeters in diameter, in which case the *total* energy is observed, and is far too high.

2. The Statistical Data

In Section V the altitude and angle dependence of large showers were calculated for several hypotheses about the primary. Table V shows the results for the altitude dependence, which are all less marked than the observed average ratio $S_{4300}/S_{3050} = 3.6 \pm 0.4$. In Fig. 9 the observed angular dependence is sharper than that predicted for primary electrons with $\gamma = 1.8$. This is, of course, in the same direction as the steeper altitude dependence.

The original calculations of the number of showers, in Table IV, show that the altitude dependence for multiple production and a zero mean free path is very much stronger than for any other case. It seems likely, therefore, that the data could be fitted by assuming multiple production and a mean free path appreciably

shorter than 200 g cm^{-2} (which was the value used in the Table V calculations). This would suggest that the showers are produced with high multiplicity, but with angular spread characteristic of normal relativistic processes rather than the large angle required by the Lewis-Oppenheimer theory.

However, in addition to the rather large statistical error in the experimental data, there are two effects which make the interpretation uncertain. The first is the change in structure function for old showers, which we have neglected, and which will affect the altitude dependence because the showers are older, on the average, at lower altitudes. The second effect is the longitudinal fluctuation in shower development. These fluctuations are known to be large,¹⁷ and will have an effect on the altitude dependence which has not been calculated.

3. A Consequence of the Meson Decay Hypothesis

If the large air showers are assumed to arise from the decay of short-lived mesons, it is clear that the existence of fully developed showers of 10^{16} ev total energy at 3050 m implies that the meson lifetime must be shorter than about 10^{-13} sec. if one assumes a single meson, or 10^{-11} sec. if one assumes a high multiplicity.

4. Primary Intensities

The values for the number of showers per square meter per hour, S , which are given in Table IV, are based on an absolute intensity extrapolated from the Heisenberg-Euler spectrum. Comparison of the resulting values of S_1 with the observed value at 3050 m shows that the assumed spectrum should be multiplied by a factor 12 to obtain an approximate fit for the primary electron hypothesis;³⁵ the best value of γ lies between 1.8 and 2.0. For the multiple production hypothesis, the factor is 10; for the single production hypothesis, the factor is 7. Thus an approximate production spectrum for electrons, in the energy range 10^{14} ev– 10^{16} ev,

³⁵ A similar calculation by Cocconi, reference 9, indicated that his experimental intensity was only 1.7 times the Heisenberg intensity. The difference arises partly because our results are in a higher energy range, and partly because his calculation neglected the finite size of the apparatus.

would be $F(E_0)$ = number of events in which energy E_0 goes into soft component = $2 \times 10^{-3} \times (10^{15} \text{ ev}/E_0)^{1.9} \text{ m}^{-2} \text{ hr.}^{-1} \text{ sterad}^{-1}$. For primary electrons this is simply the integral spectrum. For the other cases this refers to the number of events in a column of air one square meter in cross section.

Following a suggestion of H. Lewis, an attempt was made to extrapolate the meson production spectrum which can be obtained from the observed meson range spectrum³⁶ and compare this with our production spectrum, the assumption being that the large air showers arise from neutral, short-lived mesons which are produced in about the same numbers as the observed charged mesons. The extrapolation must be done differently depending on whether one assumes single or multiple production. There is a difference of a factor of about 25 between the two extrapolations, at 10^{14} ev, but uncertainties in the energy loss of the observed mesons (from density effect, possible radiation effects, and possible nuclear collisions of π -mesons) lead to an uncertainty of perhaps one power of ten in the expected number of large showers. Thus it is only possible to state that the number of showers could agree, within this large uncertainty, with either hypothesis.

VII. CONCLUSIONS

Direct measurements on large showers, with an instrument of higher resolving power than any used previously, show that they have a single core of high particle density, with the density falling off at points away from this core according to the prediction of cascade theory. The gross features of these showers therefore indicate that they are electron cascades of enormous energy. These results are not in contradiction with the finding¹⁴ that a comparatively small number of particles other than electrons or photons (penetrating charged particles and neutrons) are present in air showers. However, there is no evidence to indicate that another type of particle is responsible for the propagation or lateral spread of the electrons, and indeed it would be remarkable if a different mechanism of propagation would yield the same structure of shower as that derived from the cascade theory.

³⁶ V. C. Wilson, Phys. Rev. **53**, 337 (1938).

The fact that a unique core is observed, for showers in the energy range 10^{14} ev– 10^{17} ev, is shown to be in disagreement with the high angular divergence expected from the multiple production theory of Lewis, Oppenheimer, and Wouthuysen.²⁷ If the showers arise from neutral mesons produced in a high multiplicity, these mesons must have an average angular divergence not greater than $\sim \mu c^2/E$.

No evidence is found for showers which are narrower than normal cascade showers. The three "narrow showers" listed in Table I correspond to ordinary cascades which struck very near the apparatus. With the local shower spectrum, $S(N)$, one can estimate that this is a reasonable number of such close hits in 240 hours.

The coincidence rate between two ionization chambers at \sim zero separation, $W(\rho, 0)$, is just the particle density spectrum at a given point. This rate can be obtained by extrapolating the data of Fig. 5 (3050 m elevation) and is $W(\rho, 0) = 1.05(460/\rho)^{1.5}$ hr.⁻¹, the number of times a shower occurs which has particle density $> \rho$ particles/m² in the neighborhood of the point. The range of validity is $300 < \rho < 2000$ particles/m², but the experiments of Cocconi indicate that this expression should hold approximately at least down to 10 particles/m².

By assuming the Moliere structure function we obtain an estimate for the absolute number of showers. The local shower spectrum $S(N)$, the number of showers, containing more than N particles, whose axes cross a sphere 1 square meter in cross section, per hour, is found to be

$$S(N) = 1.8 \times 10^{-3} (N/10^6)^{-1.5} \text{ m}^{-2} \text{ hr.}^{-1}, \quad 10^5 < N < 10^6$$

$$S(N) = 1.8 \times 10^{-3} (N/10^6)^{-1.9} \text{ m}^{-2} \text{ hr.}^{-1}, \quad 10^6 < N < 10^8$$

at 3050-m elevation. The variation of number of showers with altitude is found to be more rapid, and the angular distribution more sharply vertical, than is expected on the basis of a simple analysis assuming primary electrons. However, the analysis must be refined before this can be considered to be evidence for any one type of production mechanism.

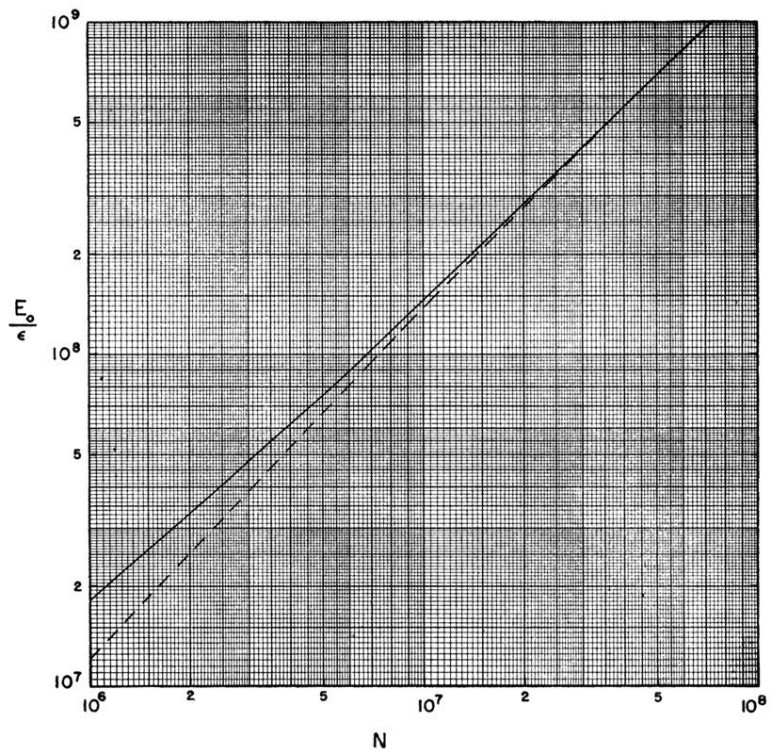
Twenty-seven showers of more than 10^{16} -ev total energy were recorded. The frequency of events of this energy agrees (very roughly) with what one obtains by extrapolating the ordinary meson spectrum, and assuming that the number of showers observed is about the same as the number of charged mesons.

ACKNOWLEDGMENTS

It is a pleasure to acknowledge the author's indebtedness to Professor Bruno Rossi, who suggested the problem and provided many helpful ideas for its execution. Much of the apparatus was designed by Mr. H. S. Bridge. The expedition at Climax was made possible by the cooperation of Mr. C. J. Abrams of the Climax Molybdenum Company, and Doctors Walter Orr Roberts and John W. Evans of the Harvard College Observatory. For the work at Doolittle Ranch the author was fortunate in having the assistance of Mr. R. J. Davisson, who carried out many of the measurements, and the cooperation of Dr. W. E. Hazen, who obtained the angular distribution data. Thanks are due to Dr. J. M. Blatt for helpful discussions concerning the analysis. The geometrical arrangement used at Doolittle Ranch was the result of a suggestion by Professor H. A. Bethe. The author is especially indebted to his wife, Janet R. Williams, for assistance in analyzing the data.

The work was supported in part by the Office of Naval Research.

FIG. 12. Energy (in critical energy units) of initiating electron vs. number of electrons created: (a) after 20 radiation units (upper curve); (b) at shower maximum (lower curve).



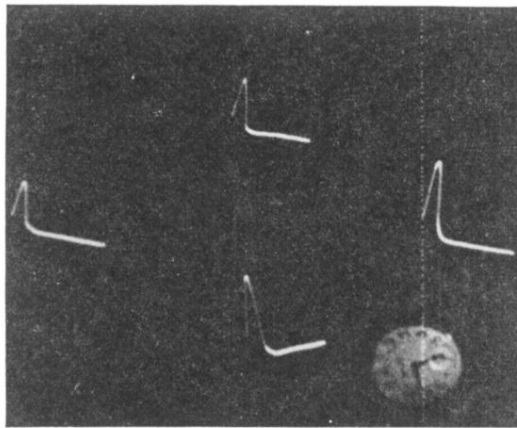


FIG. 2. Photographic record of a large air shower. Each of the four oscilloscope traces corresponds to one ionization chamber; the height of the pulse at the beginning of each trace is a measure of the particle density at that chamber. Total time of the sweep is 90 microseconds.

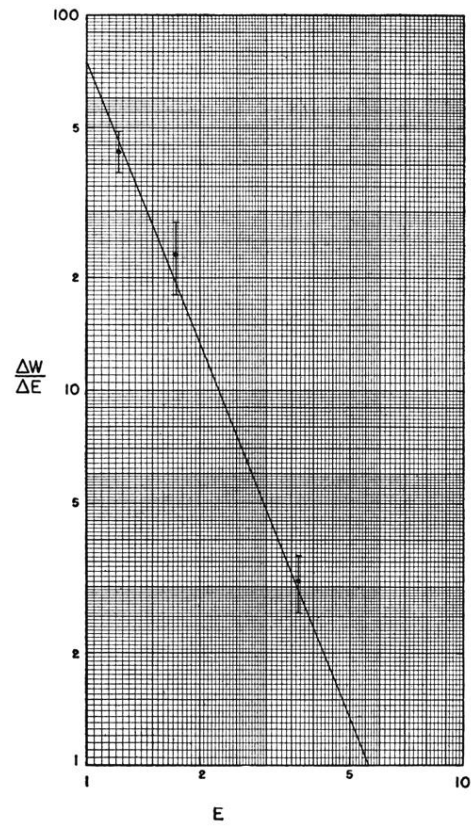


FIG. 7. Differential distribution curve of number of coincidences as function of particle density, at 0.15 m separation. E is the particle density in arbitrary units.

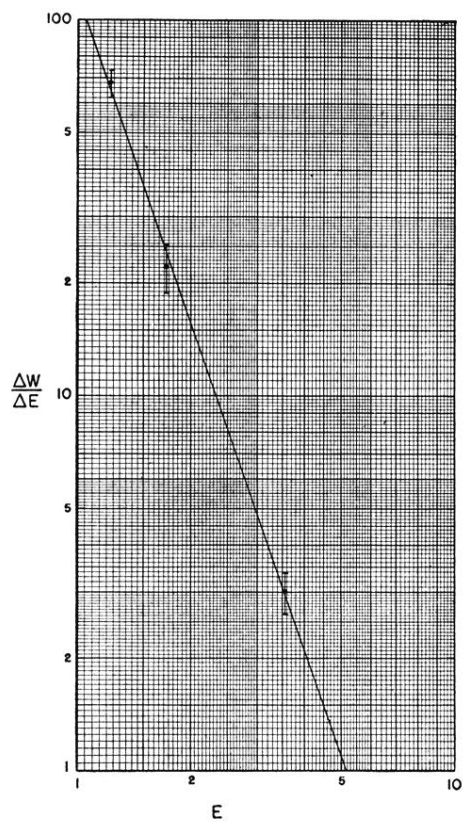


FIG. 8. Differential distribution curve at 12.2-m separation.